JOURNAL OF PURE AND APPLIED MICROBIOLOGY, Aug. 2015. Vol. **9**, p. 117-125
SPECIAL ISSUE ON RECENT RESEARCH CHALLENGES IN BIO-MEDICAL APPLICATIONS

A Computer Aided Breast Cancer Diagnosis System Based on Shearlet Moments

M. Kanchana[1] and P. Varalakshmi[2]

[1]Research Scholar, Anna University, Chennai, India.
[2]Madras Institute of Technology, Anna University, Chennai, India.

(Received: 10 February 2015; accepted: 27 April 2015)

In this paper, a computer aided breast cancer diagnosis system using Non sub sampled Shearlet Transform (NSST) is proposed. A two-step approach is developed to classify the given mammogram. At first, the given mammogram is classified into abnormal or normal followed by the classification of abnormal severity into either malignant or benign using support vector machine classifier. The proposed approach uses shearlet moments to classify the digital mammograms. From the shearlet coefficients, up to 4th order moments are computed. The results shows that the method based on shearlet moments is very robust over other multiresolutional analysis such as wavelet and curvelet transform. Also, it presents an excellent classification rate of over 90% for all considered cases.

Key words: Breast cancer, statistical moments, shearlet transform, wavelets, curvelets.

Breast cancer is the most dangerous and commonest cancer among the woman. Over 11% women get affected during their life span. A report from WHO's International Agency for Research on Cancer (IARC) says that one million breast cancer cases will happen worldwide annually and 0.4 million women die every year by breast cancer[1]. Among the various screening techniques available for breast cancer, digital mammogram by X-ray is the cheapest and best screening technique.

A computer aided classification of masses on mammograms by processing angle based and texture based features is shown in[2]. The features are assessed dependent upon gray level co-occurrence matrices for the classification of mammographic masses as benevolent or malignant. Mass lesions detection is actualized dependent upon an edge based threshold specialist methodology for the mass segmentation. From the ROI, twelve features are extracted and the classification is performed by method for an artificial neural network[3]. The questionable matter propagation through tumor masses classification framework connected in the context of mammographic images. The framework incorporates masses segmentation, features extraction and determination, and masses classification. Gullible Bayes classifier permits appointing the probability of being malignant or of being favourable to each one located mass, beginning from the qualities of the positioned features[4].

Mammogram textures might be displayed by a mixture of Gaussian distributions (GMM)[5]. The two layer architecture first gathers low level rotation invariant textural features at distinctive scales and after that takes in idle textural primitives from the gathered features by GMM. Bosom cancer images are arranged into amiable and malignant classes dependent upon Trace transform functional[6]. Follow transforms are a generalization of the radon transform where the transform

* To whom all correspondence should be addressed.
E-mail: kanchanaphd14@gmail.com

calculates functional of the picture along lines following through its pixels. New sort of classifier joining an unsupervised dependent upon an adaptive resonance theory and a managed dependent upon linear discriminant classifier model for the order of malignant and kindhearted masses on mammograms is clarified in[7].

Multi parameter methodology dependent upon non Rayleigh statistics for bosom masses in ultrasonic B-scan picture classification is illustrated in[8]. These parameters are evaluated from the site of the mass and from the boundary. Each of these parameters showed a sensible capability to separate benign and malignant masses. Another gathering method for the classification of masses in digital mammograms dependent upon neural networks with variable concealed neurons which are consolidated with hierarchical fusion is displayed in[9].

A strategy to order borders of microcalcifications as smooth and rough by utilizing the wavelet transforms is displayed in[10]. It comprises of four segments, the picture is standardized by promptly preparing, and its resolution is changed. At that point border enhancement system is connected. The low-frequency sub-band of the picture is evacuated, and the picture is recreated to the space domain with just its high frequency segments. At last the district growing algorithm is utilized to discover every conceivable microcalcification in the ensuing picture. Machine aided diagnosis framework for the programmed detection of clustered microcalcifications in digitized mammograms is displayed in[11]. It comprises of two significant steps, which are segmentation of potential microcalcification pixels and detection of singular microcalcification items utilizing feature extraction and example classification strategies.

Microcalcification (MC) detection in advanced mammogram dependent upon Support Vector Machine (SVM) is illustrated in[12]. SVM is prepared through directed figuring out how to group every area in the picture as is there MC present or MC missing. The different machine taking in methods, for example, SVM, kernel Fisher discriminant (KFD), and relevance vector machine (RVM), and advisory group machines are acknowledged for the grouping of malignant and favourable clustered microcalcifications in[13]. A methodology for MC detection is illustrated in[14] by utilizing relevance vector machine (RVM) in advanced mammograms. MC is identified at every pixel area in the computerized mammogram and an input vector is extracted to depict its encompassing picture feature. This feature is connected to two steps RVM classifier.

The texture property of tissue encompassing microcalcification (MC) clusters on mammograms for breast cancer diagnosis is illustrated in [15]. At first, images are pre-processed utilizing a wavelet based spatially adaptive method and wavelet and texture features are extracted. The extracted feature sets are thought about by method for their capability in discriminating malignant from benign tissue utilizing a PNN classifier. Discrete shearlet Transform based microcalcification order framework is exhibited in[16]. It utilizes energies extracted from the decomposed images and closest neighbour classifier for the grouping. The same features are broke down for the grouping of, mass in[17].

In this paper, breast cancer diagnosis system through computer aided design using Non sub sampled Shearlet Transform (NSST) is proposed. The rest of the paper is as follows: Section 2 introduces the methodology used in the system; NSST and SVM in a concise manner. Section 3 describes the experimental work and the obtained results are discussed in section 4. Section 5 includes the conclusion.

METHODOLOGY

In this study, the classification of breast cancer starts with extracting the suspicious regions such as microcalcification and mass based on the information provided by the MIAS database. Each extracted regions are passed through NSST with a predefined decomposition level. From the decomposed mammograms, the statistical moments of NSST coefficients are computed as features and are given to the SVM classifier. The first level classification makes a decision of the suspicious region as normal/abnormal and the second level determines the severity into benign/malignant.

Discrete Shearlet Transform

The proposed breast cancer classification system is based on discrete shearlet transform developed by Glenn Easley.et.al.,[18]. The

decomposition procedure for an image is as follows: An image consists of a finite sequence of values, $\{x[n_1,n_2]_{n_1,n_2=0}^{N-1,N-1}\}$ where $N\in !$. Identifying the domain with the finite group $\$!\,{}_N^2$, the inner product of image $\$!\,{}_N^2 \rightarrow !$ is defined as

$$(x,y) = \sum_{u=0}^{N-1}\sum_{v=0}^{N-1} x(u,v)\overline{y(u,v)} \quad ...(1)$$

Thus the discrete analog of $L^2(\mathrm{R}^2)$ is $l^2\,\mathrm{Z}\,{}_N^2$. Given an image $f \in l^2(\$!\,{}_N^2)$, let $\hat{f}[k_1,k_2]$ denote its 2D Discrete Fourier Transform (DFT):

$$\hat{f}[k_1,k_2] = \frac{1}{N}\sum_{n_1,n_2}^{N-1} f[n_1,n_2]e^{-2\prod i\left(\frac{n_1}{N}k_1+\frac{n_1}{N}k_2\right)} \quad ...(2)$$

The brackets in the equations $[\cdot,\cdot]$ denote arrays of indices, and parentheses $(\cdot,\cdot)$ denote function evaluations. Then the interpretation of the numbers $\hat{f}[k_1,k_2]$ as samples $\hat{f}[k_1,k_2] = \hat{f}(k_1,k_2)\hat{f}[k_1,k_2]$ is given by the following equation from the trigonometric polynomial.

$$\hat{f}|\xi_1,\xi_2| = \frac{1}{N}\sum_{n\cdot,n_2}^{N-1} f|n_1,n_2|e^{\ 2\|i\left(\frac{n_1}{N}\xi_1\ \frac{n_1}{N}\xi_2\right)} \quad ...(3)$$

First, to compute

$$\hat{f}(\xi_1,\xi_2)\overline{V(2^{-j}\xi_1,2^{-j}\xi_2)} \quad ...(4)$$

In the discrete domain, at the resolution level *j*, the Laplacian pyramid algorithm is implemented in the time domain. This will accomplish the multi scale partition by decomposing $f_a^{j-1}|n_1,n_2|, 0 \le n_1,n_2 < N_j - 1$, into a low pass filtered image $f_a^{j-1}[n_1,n_2]$, a quarter of the size of $f_a^{j-1}[n_1,n_2]$, and a high pass filtered image .Observe that the matrix has $f_a^{j-1}[n_1,n_2]$ size $N_j * N_l$,where $N_j = 2^{\ 2j}N$ and $f_a^0[n_1,n_2] = f[n_1,n_2]$ has size $N*N$. In particular,

$$\tilde{f}_d^j(\xi_1,\xi_2) = \hat{f}(\xi_1,\xi_2)V(2^{-2j}\xi_1,2^{-2j}\xi_2) \quad ...(5)$$

Thus, $f_a^j[n_1,n_2]$ are the discrete samples of a function $f_a^j[r_1,r_2]$, whose Fourier transform is $\tilde{f}_a^j(\xi_1,\xi_2)$.In order to obtain the directional localization the DFT on the pseudo-polar grid is computed, and then one-dimensional band-pass filter is applied to the components of the signal with respect to this grid. More precisely, the definition of the pseudo-polar co-ordinates (*u v*) εR as follows:

$$(u,v) = \left(\xi_1,\frac{\xi_2}{\xi_1}\right), if(\xi_1,\xi_2) \in D_0 \quad ...(6)$$

$$(u,v) = \left(\xi_1,\frac{\xi_1}{\xi_2}\right), if(\xi_1,\xi_2) \in D_1 \quad ...(7)$$

After performing this change of co-ordinates, is obtained and for $l = 1-2^j,.....2^j-1$:

$$f(\xi_1,\xi_2)=\overline{V(2^{-2j}\xi_1,2^{-2j}\xi_2)W_j^{(e)}(\xi_1,\xi_2)}\ \ g_j(u,v)W(2^jv-l) \quad ...(8)$$

This expression shows that the different directional components are obtained by simply translating the window function .The discrete samples are the values of the DFT of on a pseudo-polar grid. That is, the samples in the frequency domain are taken not on a Cartesian grid, but along lines across the origin at various slopes. This has been recently referred to as the pseudo-polar grid. One may obtain the discrete Frequency values of on the pseudo-polar grid by direct extraction using the Fast Fourier Trans-form (FFT) with complexityor by using the Pseudo-polar DFT (PDFT).

SVM Classifier

Support vector machines (SVMs) are a situated of related administered taking in strategies that examine data and distinguish examples, utilized for classification and regression dissection. The

standard SVM is a non-probabilistic binary linear classifier, i.e. it predicts, for every given input, which of two conceivable classes the input is a part of. A classification errand typically includes with preparing and testing data which comprises of some data cases. Each one case in the preparation set holds one "target value" (class marks) and a few "attributes" (characteristics) [19]. SVM has an additional point of interest of programmed model choice as in both the ideal number and areas of the groundwork capacities are naturally gotten throughout preparing. The execution of SVM to a great extent relies on upon the kernel.

Table 1. MIAS database images

Cases	#total images	#benign cases	#malignant cases
Normal	207	-	-
Micro calcification	25	12	13
Circumscribed masses	23	19	4
Speculated masses	19	11	8
Ill-defined masses	14	7	7
Architectural distortion	19	9	10
Asymmetry lesion	15	6	9
Total	322	64	51

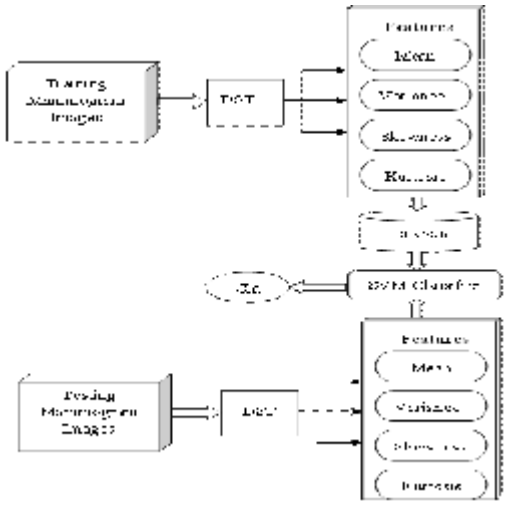

Fig. 1. Flowchart of the Proposed Mammogram Classification System

SVM is essentially a linear learning machine. For the input training sample set

$$(x_i, y_i), i = 1 \dots . n, x \, c \, R^n, y \, c\{ \quad 1, \mid 1\} \quad ...(9)$$

Let the classification hyper plane equation is to be

$$(w, x) + b - 0 \quad ...(10)$$

Thus the classification margin is .To maximize the margin, that is to minimize ,the optimal hyperplane problem is transformed to quadratic programming problem as follows,

$$\begin{cases} min\phi(\omega) - \frac{1}{2}(\omega, \omega) \\ s.t. \, y_i[(\omega.x) - b] > 1, \quad i - 1,2 \dots \dots . i \end{cases} \quad ...(11)$$

After introduction of Lagrange multiplier, the dual problem is given by,

$$\begin{cases} \max \; Q(\alpha) = \sum_i^n {}_1 \alpha_i \quad \frac{1}{2} \sum_i^n {}_1 \sum_j^n {}_1 y_i y_j \alpha_i \alpha_j K(x_i . x_j) \\ s.t. \sum_{i=1}^m y_i \alpha_i - 0, \quad \alpha_i > 0, \quad i - 1,2 \dots \dots \dots , n \end{cases} \quad ...(12)$$

According to Kuhn-Tucker rules, the optimal solution must satisfy

$$\alpha_i \left(y_i ((w . x_i) + b) \right) - 1 - 0, i - 1,2 \dots \dots . n \quad ...(13)$$

Table 2. Classification Accuracy Rates of Normal And Abnormal Cases By Shearlet Moments

#Directions	Classification rate (%)					
	Level 2		Level 3		Level 4	
	Normal	Abnormal	Normal	Abnormal	Normal	Abnormal
2	77.14	64.35	80	65.22	77.14	68.70
4	80	60.87	84.29	66.96	87.14	69.57
8	85.71	66.96	88.57	85.22	91.43	92.17
16	85.71	86.96	84.29	86.96	84.29	86.96
32	87.14	86.09	82.86	81.74	81.43	83.48
64	81.43	84.35	80	86.96	87.14	85.22

That is to say if the option solution is

$$\alpha^* \quad (\alpha_1^*, \alpha_2^* \ldots\ldots\ldots, \alpha_l^*)^T \qquad i \quad 1, 2 \ldots\ldots\ldots\ldots n$$

...(14)

Then

$$w^* = \sum_{i-1}^{n} \alpha_i^* y_i x_i$$

$$b^* - y_i - \sum_{i-1}^{n} y_i \alpha_i^* (x_i . x_j), j \in \{j | \alpha_i^* > 0\}$$

....(15)

For every training sample point, there is a corresponding Lagrange multiplier. And the sample points that are corresponding to don't contribute to solve theclassification hyper plane while the other points that are corresponding to do, so it is called supportvectors. Hence the optimal hyperplane equation is given by,

$$\sum_{x_i \in SV} \alpha_i y_i (x_i . y_i) + b = 0 \qquad ...(16)$$

The hard classifier is then,

Table 3. Classification accuracy rates of normal and abnormal cases by wavelet and curvelet moments

#Level	Classification rate (%)							
	Wavelet							
	db8		sym8		bior3.7		Curvelet	
	Normal	Abnormal	Normal	Abnormal	Normal	Abnormal	Normal	Abnormal
2	82.86	68.70	81.43	60.87	81.43	64.35	84.29	63.48
3	87.14	64.35	72.86	71.30	82.86	68.70	82.86	83.48
4	78.57	73.04	82.86	77.39	85.71	80.00	87.14	89.57
5	84.29	76.52	87.14	81.74	87.14	86.09	85.71	89.57
6	81.43	78.26	85.71	82.61	84.29	88.70	82.86	85.22

Table 4. Classification Accuracy Rates of Benign And Malignant Cases Using Shearlet Moments

# Directions	Classification rate (%)					
	Level 2		Level 3		Level 4	
	Benign	Malignant	Benign	Malignant	Benign	Malignant
2	53.12	64.70	51.56	68.62	60.93	68.62
4	54.68	78.43	71.87	74.50	76.56	76.47
8	76.56	86.27	**95.31**	**90.19**	87.5	88.23
16	84.37	80.39	87.5	78.43	89.06	80.39
32	87.5	80.39	82.81	76.47	82.81	82.35
64	84.37	80.39	84.37	78.43	84.37	82.35

Table 5. Classification accuracy rates of benign and malignant cases using wavelet and curvelet moments

#Level	Classification rate (%)							
	Wavelet							
	db8		sym8		bior3.7		Curvelet	
	Benign	Malignant	Benign	Malignant	Benign	Malignant	Benign	Malignant
2	59.38	64.71	70.31	70.59	65.63	66.67	65.63	54.90
3	62.50	76.47	68.75	78.43	67.19	68.63	76.56	76.47
4	78.13	80.39	81.25	80.39	79.69	76.47	81.25	80.39
5	87.50	72.55	82.81	78.43	81.25	80.39	85.94	88.24
6	93.75	76.47	89.06	82.35	90.63	80.39	87.50	82.35

$$y = sgn\left[\sum_{x \in SV} \alpha_i y_i (x_i \cdot y_i) + b\right] \quad ...(17)$$

For nonlinear situation, SVM constructs an optimal separating hyperplane in the high dimensional space by introducing kernel function hence the nonlinear SVM is given by,

$$\begin{cases} \min \phi(\omega) = \frac{1}{2}(\omega, \omega) \\ s.t.\ y_i((\omega \cdot \phi(x_i)) + b) \geq 1, \quad i = 1, 2, \ldots, l \end{cases} \quad ...(18)$$

And its dual problem is given by,

$$\begin{cases} \max L(\alpha) = \sum_{i=1}^{l} \alpha_i - \frac{1}{2}\sum_{i=1}^{l}\sum_{j=1}^{l} y_i y_j \alpha_i \alpha_j K(x_i, x_j) \\ s.t. \sum_{i=1}^{n} y_i \alpha_i = 0, \quad 0 \leq \alpha_i \leq C, \quad i = 1, 2, \ldots, n \end{cases} \quad ...(19)$$

Thus the optimal hyperplane equation is determined by the solution to the optimal problem.

EXPERIMENTAL

Database

In this study, Mammographic Image Analysis Society (MIAS) database is selected for performance analysis as it is commonly used for similar research work[20]. Also it includes various cases of abnormality. The distribution of different cases available in MIAS database is shown in Table 1. There are 322 mammogram images of left and right breast acquired from 161 patients. As the main objective of the proposed approach is to detect the abnormal severity into benign or malignant, all the benign (64 images) and malignant images (51 images) are considered for this study irrespective of the type of abnormalities. From the vast number of normal images in the database, only 70 images are considered and are randomly chosen.

Feature Extraction

As the classifier accuracy heavily depends on the extracted features, the main functional step in any classification system is feature extraction. In the proposed approach, Non sub sampled Shearlet Transform (NSST) is used to extract the features from the mammograms. The main reason to use NSST is that its advanced directional sensitivity over discrete wavelet transforms and of various shapes. Also, it is very effective in signals that contain distributed discontinuities such as edges in comparison with wavelets. The proposed mammogram classification system based on NSST is shown in Figure 1

The proposed approach aims at distinguishing between the normal and abnormal mammogram images and determining the abnormalities into either benign or malignant. In order to tackle these analyses, a two phase integrated analysis is developed. In the first phase, the given mammogram image is analyzed for the abnormalities that exists in the given mammogram based on the features extracted from the NSST transformed image. As NSST is a multi-scale directional representation of an image, it produces high dimensional data i.e., huge number of shearlet coefficients which depends on the decomposition level and number of directions. In the feature extraction stage, the shearlet coefficients are processed in order to extract a feature set with compact representation of that image. This can be achieved by taking the statistical parameters from the shearlet coefficients.

Glenn Easley et.al,[18] stated that the shearlet coefficients can be modeled as generalized Gaussian distributions. The close relationship of Gaussian models with variance, entropy and energies[21] guide the use of lower order moments as important features. Also, the high order moments are employed to consider the unknown

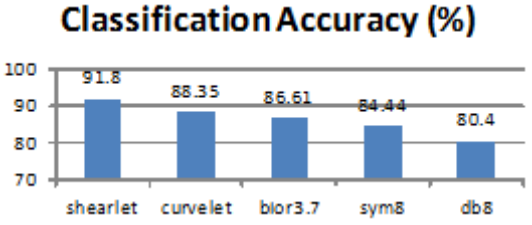

Fig. 2. Maximum Classification Accuracy Obtained For the Classification Of Normal And Abnormal Cases

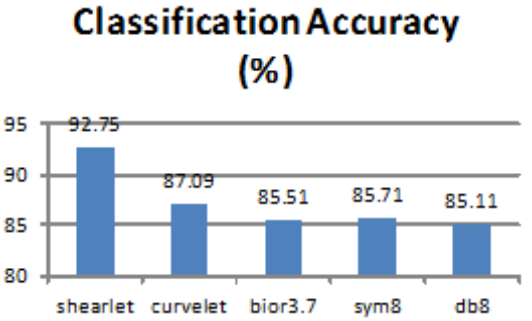

Fig. 3. Maximum Classification Accuracy Obtained For the Classification Of Benign and Malignant Cases

distributions of shearlet coefficients. Hence, the shearlet moments of 1st, 2nd, 3rd and 4th order are used as features. In the second phase, the same shearlet moments are used for the classification of abnormal severity into either benign or malignant. The extracted features for the decomposed image *I* are as follows:

$$First\ Movement\ \bar{\mu}_s = \frac{1}{RC}\sum_{i=1}^{R}\sum_{j=1}^{C} I_s(i,j) \quad ...(20)$$

$$Second\ Movement\ \sigma_s = \frac{1}{RC}\sum_{i=1}^{R}\sum_{j=1}^{C}(I_s(i,j) - \bar{\mu}_s)^2 \quad ...(21)$$

$$Third\ Movement\ \gamma_s = \frac{1}{RC}\sum_{i=1}^{R}\sum_{j=1}^{C}\left[\frac{I_s(i,j)-\bar{\mu}_s}{\sigma_s}\right]^3 \quad ...(22)$$

$$Fourth\ Movement\ k_s = \frac{1}{RC}\sum_{i=1}^{R}\sum_{j=1}^{C}\left[\frac{I_s(i,j)-\bar{\mu}_s}{\sigma_s}\right]^4 - 3 \quad ...(23)$$

where I_s is the s^{th} sub-band of the decomposed image *I*, *R* and *C* is the height and width of the corresponding sub-band. In this study, the extracted shearlet moments are fed into SVM classifier for classification in each phase. The first phase SVM classifier is trained by using normal and abnormal shearlet moments and the second phase SVM classifier is trained by using benign and malignant shearlet moments of training mammogram images. If the classified output of the first phase SVM classifier for an unknown mammogram is abnormal then the second phase SVM classifier is triggered to classify the abnormal severity into benign or malignant.

RESULTS AND DISUCSSION

The first step in the proposed integrated approach for breast cancer classification based on NSST is to test the unknown image which is to be classified as normal or abnormal. The obtained classification accuracy of normal vs. abnormal cases is shown in Table 2. As NSST is multi-scale directional representation, the proposed approach is tested up to 4th level of decomposition with maximum of 64 directions. The proposed approach considers 64 benign, 51 malignant and randomly selected 70 normal images for evaluation. In order to decrease mortality due to breast cancer, an efficient and accurate classification system is required to detect breast cancer earlier. To design such a system, only two-class problem is considered. Hence in the first step, the benign and malignant images are grouped and marked as abnormal cases and in total 115 images. The SVM classifier is trained by using 2/3rd of images in each category.

Table 2 illustrated that the maximum average classification accuracy achieved for the first step of the proposed approach is 91.8% at 4th level decomposition and 8 directions. In order to compare the effectiveness of NSST over wavelet and curvelet transform, the proposed moments are extracted using wavelet and curvelet coefficients and classification accuracy is evaluated and tabulated in Table 3. The maximum accuracy achieved by curvelet transform is 88.35% while the maximum average accuracy obtained by three wavelet functions such as db8, bior3.7 and sym8 is 86.61%. The maximum average classification accuracy achieved by the first step is shown in Figure 2.

The abnormalities detected in the first step of the proposed approach are again classified into their abnormal severity as benign or malignant for better treatment. Table 4 lists the maximum average classification accuracy achieved by the proposed approach. For shearlet moments, the average classification accuracy obtained is 92.75% at 3rd level decomposition with 8 directions. For curvelet and wavelet moments, the maximum accuracy obtained is 87.09% and 85.71% respectively

The results suggest that the shearlet moments perform better than wavelet and curvet moments. Also, the curvelet moments are better than wavelet moments as it captures the multidimensional features in wedges. The maximum average classification accuracy achieved for the second step of the proposed approach is shown in Fig 3.

CONCLUSION

An efficient approach for breast cancer diagnosis based on NSST and SVM classifier is presented. NSST at different scales and directions is used to decompose the given mammogram for feature extraction, then extracting the shearlet moments from the decomposed image as features. The effectiveness of the proposed system is analyzed on MIAS database images and compared to wavelet and curvelet based moments. The obtained maximum classification rate using shearlet moments for normal and abnormal is 91.8% and 92.75% for benign and malignant cases. The comparative study with curvelet and wavelet shows that the shearlet moments yield higher classification accuracy than wavelet and curvelet moments.

REFERENCES

1. Eltoukhy, Mohamed Meselhy, Ibrahima Faye, and BrahimBelhaouari Samir. "Breast cancer diagnosis in digital mammogram using multiscale curvelet transform." *Computerized Medical Imaging and Graphics*, 2010; **34**(4): 269-276.
2. Mudigonda, Naga R., R. Rangayyan, and JE Leo Desautels. "Gradient and texture analysis for the classification of mammographic masses." Medical Imaging, *IEEE Transactions on*, 2000; **19**(10): 1032-1043.
3. Cascio, D. O. N. A. T. O., Francesco Fauci, Rosario Magro, Giuseppe Raso, Roberto Bellotti, Francesco De Carlo, Sonia Tangaro et al. "Mammogram segmentation by contour searching and mass lesions classification with neural network." Nuclear Science, *IEEE Transactions on*, 2006; **53**(5): 2827-2833.
4. Marcello Salmeri, Giulia Rabottino, and SimonaSalicone. "Metrological characterization of a CADx system for the classification of breast masses in mammograms." Instrumentation and Measurement, *IEEE Transactions on*, 2010; **59**(11): 2792-2799.
5. Biswas, Sujoy Kumar, and Dipti Prasad Mukherjee. "Recognizing architectural distortion in mammogram: a multiscale texture modeling approach with GMM." Biomedical Engineering, *IEEE Transactions on*, 2011; **58**(7): 2023-2030.
6. Ganesan, Karthikeyan, U. RajendraAcharya, Chua Kuang Chua, Choo Min Lim, and K. Thomas Abraham. "One-Class Classification of Mammograms Using Trace Transform Functionals." 1-1.**63**(2).pp: 304 – 311.
7. Hadjiiski, Lubomir, BerkmanSahiner, Heang-Ping Chan, Nicholas Petrick, and Mark Helvie. "Classification of malignant and benign masses based on hybrid ART2LDA approach." Medical Imaging, *IEEE Transactions on*, 1999; **18**(12): 1178-1187.
8. Shankar, P. Mohana, Vishruta A. Dumane, Catherine W. Piccoli, John M. Reid, Flemming Forsberg, and Barry B. Goldberg. "Computer-aided classification of breast masses in ultrasonic B-scans using a multiparameter approach." Ultrasonics, Ferroelectrics and Frequency Control, *IEEE Transactions on*, 2003; **50**(8): 1002-1009.
9. Panchal, Rinku, and BrijeshVerma. "Neural classification of mass abnormalities with different types of features in digital mammography." *International Journal of Computational Intelligence and Applications*, 2006; **6**(1): 61-75.
10. Docusse, Tiago A., Aledir S. Pereira, and NorianMarranghello. "Microcalcification border characterization." Engineering in Medicine and Biology Magazine, *IEEE*, 2009; **28**(5): 41-43
11. Yu, Songyang, and Ling Guan. "A CAD system for the automatic detection of clustered microcalcifications in digitized mammogram films." Medical Imaging, *IEEE Transactions on*, 2000; **19**(2): 115-126.
12. El-Naqa, Issam, Yongyi Yang, Miles N. Wernick, Nikolas P. Galatsanos, and Robert M. Nishikawa. "A support vector machine approach for detection of microcalcifications." Medical Imaging, *IEEE Transactions on*, 2002; **21**(12): 1552-1563.
13. Wei, Liyang, Yongyi Yang, Robert M. Nishikawa, and Yulei Jiang. "A study on several machine-learning methods for classification of malignant and benign clustered microcalcifications." Medical Imaging, *IEEE Transactions on*, 2005; **24**(3): 371-380.
14. Wei, Liyang, Yongyi Yang, Robert M. Nishikawa, Miles N. Wernick, and Alexandra Edwards. "Relevance vector machine for automatic detection of clustered microcalcifications." Medical Imaging, *IEEE Transactions on*, 2005; **24**(10): 1278-1285.
15. Karahaliou, Anna N., Ioannis S. Boniatis, Spyros G. Skiadopoulos, Filippos N. Sakellaropoulos, Nikolaos S. Arikidis, Eleni A. Likaki, George S. Panayiotakis, and Lena I. Costaridou. "Breast cancer diagnosis: analyzing texture of tissue surrounding microcalcifications." information Technology in Biomedicine, *IEEE Transactions on*, 2008; **12**(6): 731-738.

16. Ali, J. Amjath, and J. Janet. "Discrete Shearlet Transform Based Classification of Microcalcification in Digital Mammograms." *Journal of Computer Applications (JCA),* 2013; **6**.1.
17. Amjath Ali, J., and J. Janet. "Mass Classification In Digital Mammograms Based On Discrete Shearlet Transform." *Journal of Computer Science,* 2013; **9**.6.
18. Easley, Glenn, Demetrio Labate, and Wang-Q. Lim, "Sparse directional image representations using the discrete shearlet transform." *Applied and Computational Harmonic Analysis,* 2008; **25**.1: 25-46.
19. Smola A. J., Scholkopf B., and Muller K. R., "The connection between regularization operators and support vector kernels", *Neural Networks New York,* 1998; 11: pg 637-649.
20. MIAS Database: http://peipa.essex.ac.uk/pix/mias/
21. Starck, J. L., F. Murtagh, and R. Gastaud. "A new entropy measure based on the wavelet transform and noise modeling." *Ieee Transactions on Circuits and Systems Part 2 Analog and Digital Signal Processing,* 1998; **45**: 1118-1124.